research papers

A wide-aperture dynamically focusing sagittal monochromator for X-ray spectroscopy and diffraction

R. L. Bilsborrow,* P. A. Atkinson, N. Bliss, A. J. Dent,‡ B. R. Dobson and P. C. Stephenson

CCLRC Daresbury Laboratory, Daresbury, Warrington WA4 4AD, UK.
E-mail: r.l.bilsborrow@dl.ac.uk

A scanning dynamically focusing sagittal X-ray monochromator accepting 7 mrad of the fan from a 6 T wiggler is in routine use on beamline 16.5 (ultra-dilute spectroscopy) of the SRS at CCLRC Daresbury Laboratory, UK. The energy range covered is 7–27 keV, with a horizontal spot size of <1.1 mm FWHM. Measured monochromatic flux from a Si 220 crystal pair is 1×10^{11} photons s^{-1} (100 mA)$^{-1}$ at 9 keV. This level of flux, usually associated with an insertion device on a third-generation source, permits collection of EXAFS data on concentrations at or below 10 ppm.

Keywords: X-ray monochromator; wide aperture; sagittal focus; dynamic focus; X-ray spectroscopy.

1. Introduction

The SRS is a second-generation source operating at 2 GeV. Station 16.5 is dedicated to dilute X-ray absorption spectroscopy (EXAFS and XANES) in the range 7–40 keV, with horizontal focus available up to 27 keV. The station accepts 7 mrad of the fan from a 6 T superconducting single-period wiggler, equivalent to a beam width of 135 mm at the monochromator. The optical configuration follows the now familiar pattern of collimating mirror, double-crystal monochromator and vertically focusing mirror, with the source-to-monochromator and monochromator-to-sample distances being in the ratio 3:1. The 1.2 m ultra-low-expansion glass (Rockwell) mirrors are plane and are bent vertically for collimation/vertical focus. Horizontal focus is achieved by means of a scanning sagittally focusing double-crystal monochromator.

On a station covering such a wide energy range it is highly desirable to have the option of adjusting the mirror angle(s) to optimize harmonic rejection at the working energy. This mode of operation is not possible when a mirror also performs the function of horizontal focus, as the ground-in sagittal curvature requires it to operate at a fixed angle of incidence. The freedom from this constraint easily justifies the additional complexity of a focusing monochromator. Sagittal focus, harmonic rejection and correction for crystal twist are all adjusted dynamically during scanning.

‡ Present address: Diamond Light Source Ltd, Diamond House, Chilton, Didcot, Oxfordshire OX11 0DE, UK.

2. Sagittally focusing monochromator

The first crystal is water cooled, having a single water channel fed from a chiller unit. A gravity feed from a header tank is used to minimize mechanical vibration.

2.1. Horizontal acceptance

The horizontal divergence, w, intercepted by a double-crystal monochromator with sagittally bent second crystal has been shown to be (Hrdy, 1992)

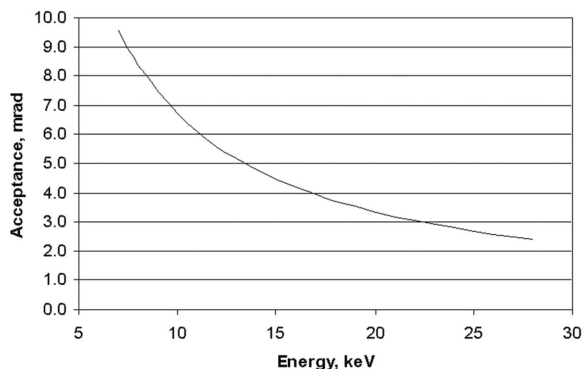$$w = 2(\Delta\theta \sin 2\theta)^{1/2}, \tag{1}$$

where θ is the Bragg angle and $\Delta\theta$ is the rocking-curve width. The transmission efficiency is shown to be 0.67 as compared with two flat crystals. This energy dependence of w results in an acceptance that, at 7 keV, is greater than the monochromator aperture, falling to 2.5 mrad at 27 keV (Fig. 1).

2.2. Horizontal focus

There are several approaches to achieving sagittal focus by bending a second crystal. These can loosely be divided into (a) thick (stiff) crystals with deep slots that act as hinges (Yoneda et al., 2001) and (b) thin (flexible) crystals with some means of minimizing anticlastic bending. This usually takes the form of stiffening ribs on the rear face (Sparks et al., 1982).

The first type, when bent, produces a polygonal section and clearly the focal spot size is limited to the size of the individual segments. Increasing the number of slots, even up to the limiting case of equal slot and segment widths (the comb

Figure 1
Horizontal acceptance of a double-crystal $(n, -n)$ monochromator with sagittally bent second crystal (Hrdy, 1992). The upper limit corresponds to a radius of curvature of 1.05 m, the minimum radius that the bending mechanism can achieve.

structure), reduces the spot size but incurs a severe penalty: the surfaces above the slots and those above the thick segments cannot reflect simultaneously so that the flux is reduced by up to 50%. This is due to the fact that the variation in the compressive stress between the thick and thin sections alters the lattice parameter so that their respective rocking curves do not overlap. Of course this effect also applies in the second case, where there is no reflection from the area above any stiffening ribs, but this area is small compared with the total reflecting area.

We have employed a 'thin crystal' approach, but rather than depending on stiffening ribs we have followed the principle established by Kushnir *et al.* (1993). They have shown that the anticlastic curvature of a simply supported isotropic crystal is zero at the centre of the crystal, provided that the crystal's aspect ratio is equal to a 'golden value' dependent on the Poisson coefficient v. For Si this ratio is ~6.6:1, the long axis being the axis of anticlastic curvature. In order to maintain this ratio whilst keeping the length to manageable proportions, the crystal is divided into eight segments. Each segment is separated from its neighbours by deep ribs on the rear face so that the segments behave effectively as a contiguous array of distinct crystals. It is important to appreciate that these are not stiffening ribs in the usual sense: their role is solely to define the width of the minor axis of the crystal segments. For satisfactory performance we have found by experiment that the thickness variation of the diffracting surface (excluding the ribs) must not exceed 2%. If this value is exceeded then variations in radius of curvature across the width result in an expanded focal spot, a non-Gaussian intensity profile and some loss of intensity (not all segments are evenly illuminated). In the worst case (variation >5%) it was not possible to achieve reflection from more than 30% of the total width at any one time. The first two crystals tested were Si $\langle 311 \rangle$ cut, chosen because the $\langle 622 \rangle$ reflection is forbidden. However, the next two, including the one now in use, are $\langle 220 \rangle$. The reasons for this choice are twofold. Firstly, in both of the $\langle 311 \rangle$ crystals tested severe and non-normalizing glitches appeared in experimental data near the Pt and Hg L_{III} absorption edges making dilute measurements on these elements impossible.

Secondly, a $\langle 311 \rangle$ crystal of this width cannot be cut from a standard Si boule as used in the semiconductor industry. This makes replacements expensive and greatly extends delivery times. Furthermore, the presence of two mirrors, at least one of which is always adjusted to have its reflectivity cut off just above the working energy, means that higher harmonic output from the monochromator is not a serious hindrance. All of our crystals were produced by Crystal Scientific (UK) (Alnwick, Northumberland, UK).
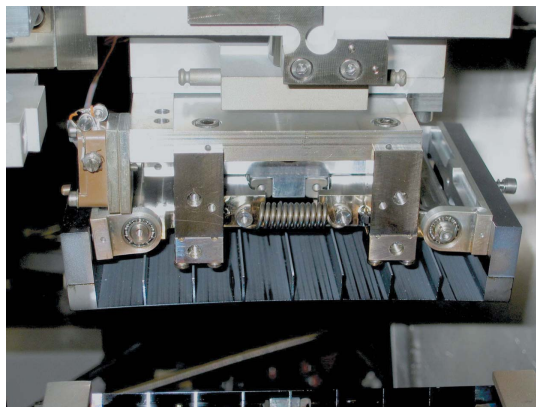
2.3. The bending mechanism

Fig. 2 shows a view of the sagittal crystal and bending mechanism as seen from the source. The crystal is suspended from the bending mechanism by a simple three-point arrangement of pins through the side arms. Bending is achieved by means of a stepper-motor-driven ball-screw that drives a wedge along precision linear roller bearings. The wedge pushes apart two blocks, held together by springs that bear on the crystal side arms *via* two additional pieces that are free to rotate on ball bearings. This arrangement is shown schematically in Fig. 3. (The springs and supporting structures are omitted for clarity.)

The increase in curvature during bending results in a small change in the separation between the first and second crystals, and hence exit beam height. At higher energies this makes a larger contribution to the variation in exit beam height than does the variation with Bragg angle. The beam position on the sample can be maintained either by changing the crystal separation dynamically during the scan (constant exit height mode) or, provided the second mirror is at a sufficiently high angle to allow some beam movement, by translating the sample stage vertically.

### 2.4. Adjustment of the sagittal crystal

In addition to the bending mechanism, the position and orientation of the crystal is adjustable by the following stepper motor drives:

(i) Horizontal displacement along beam axis. This allows the beam from the first crystal to intercept the second crystal near

Figure 2
View of the sagittal crystal and bending mechanism as seen from the source.
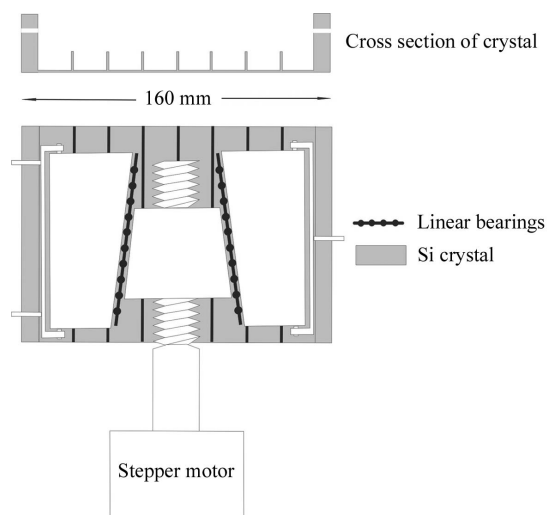
Figure 3
Sagittal crystal and bending mechanism.

to its centre, the 'sweet zone' where anticlastic bending is at a minimum. The displacement is set to suit the Bragg angle for the absorption edge being measured. It is not adjusted during scans as the amount by which the beam footprint moves along the crystal is small in relation to the length of the crystal.

(ii) Vertical displacement (separation) from first crystal. This may be adjusted dynamically during scans to maintain constant exit beam height. It is also used to extend the angular range over which the beam can be brought to the centre of the crystal. At high angles the gap needs to be increased to prevent the crystal from intercepting the incoming beam from the collimating mirror. At lower angles the separation is reduced. (A fixed separation would require an unreasonably long horizontal travel.)

(iii) Roll about beam axis. This is adjusted to remove any sideways deflection of the beam. When correctly set, there is no horizontal displacement of the focal spot as the Bragg axis is scanned. It is not adjusted during scans.

(iv) Pitch (rotation about the Bragg axis). This is used to optimize the reflection from the second crystal and to detune for harmonic rejection. There are two drive mechanisms: a stepper-motor-driven lead screw for coarse adjustment and, riding on this, a piezo-electric actuator for fine adjustment and harmonic rejection. This actuator forms part of a servo loop to maintain constant harmonic rejection during the scan.

(v) Yaw about beam axis. When a crystal is cylindrically bent, then in order to satisfy the condition for Bragg reflection over the full width the axis of the cylinder must be parallel to the beam direction. Imperfections in the bending mechanism, and/or dimensional variations in the crystal can result in a twist being applied as the crystal is bent, so that the axis of the cylindrical section produced is no longer parallel with the beam direction. In this condition it is not possible for the full width of the crystal to reflect simultaneously. The result is a reflection whose width is inversely proportional to the degree of twist and which moves across the crystal with adjustments in pitch. Provided that the distortion is small and takes the form of a simple twist, then a movement of the yaw axis to bring the

cylindrical axis parallel with the incoming beam will allow the full width of the crystal to reflect. When this condition is achieved, movements of the pitch axis result in a uniform variation in reflected intensity across the entire crystal.

2.5. Operation

The Bragg axis is moved to the start of the scan and the second crystal is translated horizontally and vertically as required to centre it on the reflected beam from the first crystal. Pitch is adjusted to maximize intensity, and the beam profile is imaged by means of a fluorescent screen, positioned at the focal point, and a CCTV camera. The bend is then increased in stages, accompanied by pitch adjustments to maintain intensity. As focus is approached, small movements in yaw are made to ensure that the entire crystal is reflecting and that intensity is maximized. A number of bend/pitch/yaw/pitch iterations are required to achieve the minimum spot size and maximum intensity. The bend and yaw motor positions thus found are entered into the dynamic focus software. The Bragg axis is moved to the end of the scan and the optimum bend and yaw positions are again established and entered. The software then performs an interpolation to determine the bend and yaw positions required for each point in the scan. It is often found that no alteration of the yaw position is necessary.
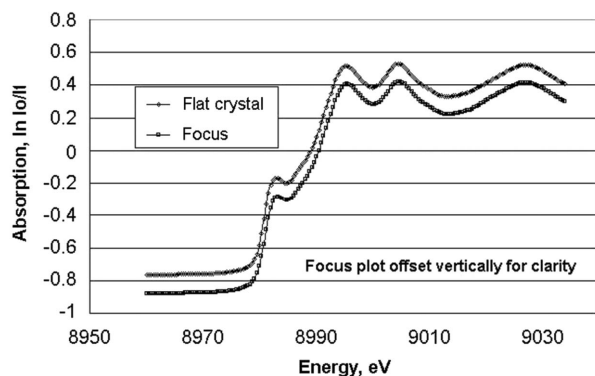
2.6. The servo system

In order to maintain beam intensity and constant higher harmonic rejection a servo system operates on the pitch axis. This is implemented in software and operates after the motor moves for each data point are complete. Once the required tolerance (measured-reference) is reached, data acquisition commences. No further adjustments are made during this period. A tolerance of $\pm 0.5\%$ is used. A smaller tolerance results in increased dead-time with no improvement in the signal-to-noise ratio.

2.6.1. Servo operation. The analogue voltage from the incident ion chamber amplifier is fed to an ADC and compared with the reference value and, if it is outside the tolerance, a calculated movement of the piezo pitch motor is made. Usually two iterations are sufficient. The reference values are established by a routine that scans the pitch axis over the rocking curve at the end, and then the start of the angular range of the scan, with the appropriate bend and yaw positions set. A Gaussian fit is applied to each curve and a linear interpolation performed after allowing for the required amount of de-tuning for higher harmonic rejection. During multiple scanning this routine is performed automatically at the start of each scan. There is an option to apply a correction for beam decay when beam lifetimes are very short. For typical beam lifetimes with a half life of 20 h or more this option is not needed.

2.6.2. Dead-time. When scanning there is an additional dead-time penalty of approximately 2.5 s per data point compared with the unfocused mode. However, this is a small
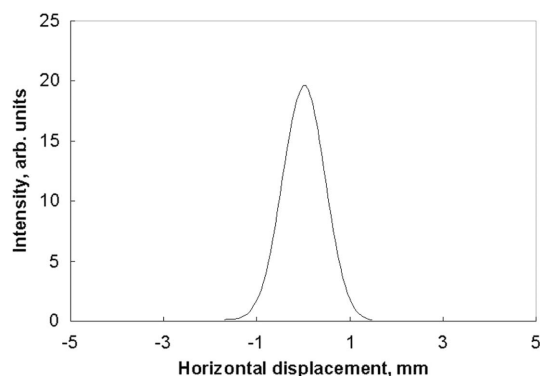
Figure 4
Horizontal profile of the focal spot at 26 keV.

Figure 5
Cu-foil XANES spectra with and without focus.

Table 1
Sagittally focusing monochromators at SRS stations.

Station	Source	Energy range (keV)	Aperture (mrad)	Technique
7.1	Bending magnet	4–10	3.3	XAS
6.2	Multipole wiggler	4–18	4.5	SAXS/WAXS
10.1	Multipole wiggler	5–13.5	3.5	MAD (Cianci *et al.*, 2005)

Figure 6
(*a*) Ag foil EXAFS. (*b*) Background-subtracted and k^3-weighted spectrum.

price to pay for the substantial gains in flux which are typically a factor of ten or more, depending on sample size.

The typical time for a single EXAFS scan is 30–50 min in total.

3. Performance

At 27 keV (2.5 mrad acceptance) the measured flux gain compared with the flat crystal condition is within 3% of the expected value, calculated from: flux from flat crystal with 10 mm (0.58 mrad) beam width $\times$ (2.5/0.58) $\times$ 0.67, where 0.67 is the transmission efficiency of a bent crystal. The small loss arises from the reduced reflectivity from the areas above the ribs behind the diffracting surface that are included with the wider aperture.

An intensity profile, obtained by scanning a 20 µm slit through the beam at the focus in 0.1 mm steps is shown in Fig. 4. The horizontal width is 1.1 mm FWHM over the entire working range.

XANES spectra recorded at the Cu *K*-edge both with and without focus are shown in Fig. 5. Note that there is no discernible loss in resolution.
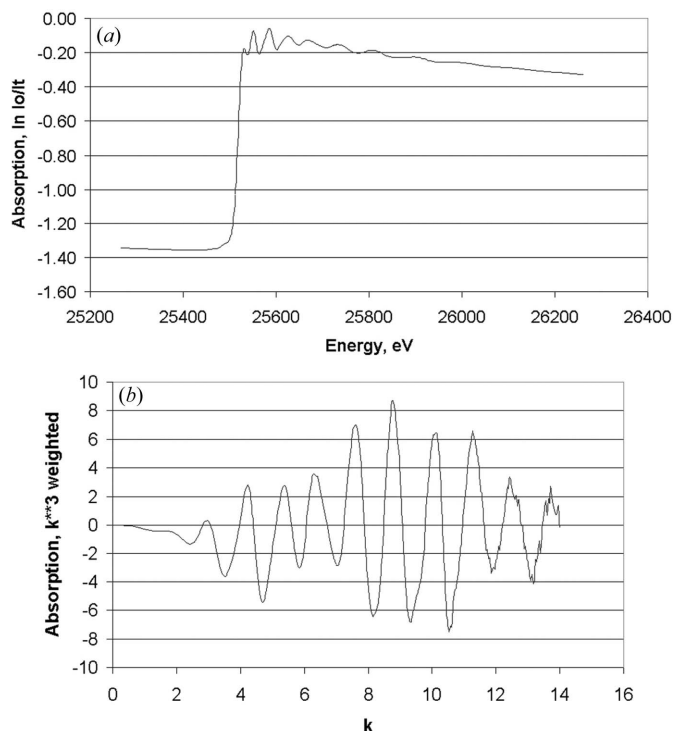
Figs. 6(*a*) and 6(*b*) show an Ag foil EXAFS scan, together with the background-subtracted and k^3-weighted spectrum.

3.1. Stability

Over 15 consecutive 50 min EXAFS scans are routinely collected, the run only being terminated by the next machine refill. Bend and yaw values, once determined for a given energy range, may be saved and read in at a later date. Although the bend values are perfectly reproducible, the yaw often requires a small adjustment after large changes to the bend radius, such as are required when moving between widely separated absorption edges.

4. Other installations

Following the successful commissioning on station 16.5, sagittally focusing monochromators of this type, albeit with narrower apertures, have since been installed on various other stations on the SRS at Daresbury (see Table 1). On the diffraction stations the narrower apertures keep $\Delta\lambda/\lambda < 10^{-3}$.

5. Conclusions

For a beamline requiring rapid access to a broad energy range a sagittally focusing monochromator offers distinct advantages over a fixed torroidal mirror. Such a device greatly extends the capability and useful life of beamlines on a mature source.

Furthermore, on third-generation sources where space on insertion-device beamlines is at a premium, a wide-aperture focusing monochromator on a bending magnet can provide a viable alternative.

References

Cianci, M., Antonyuk, S., Bliss, N., Bailey, M. W., Buffey, S. G., Cheung, K. C., Clarke, J. A., Derbyshire, G. E., Ellis, G. E., Enderby, M. J., Grant, A. F., Holbourn, M. P., Laundy, D., Nave, C., Ryder, R., Stephenson, P., Helliwell, J. R. & Hasnain, S. S. (2005). *J. Synchrotron Rad.* **12**, 455–466.

Hrdy, J. (1992). *Rev. Sci. Instrum.* **63**, 914–915.

Kushnir, V. I., Quintana, J. P. & Georgopoulos, P. (1993). *Nucl. Instrum. Methods*, A**328**, 588–591.

Sparks, C. J., Ice, G. E., Wong, J. & Batterman, B. W. (1982). *Nucl. Instrum. Methods*, **172**, 237–242.

Yoneda, Y., Matsumoto, N., Furukawa, Y. & Ishkawa, T. (2001). *J. Synchrotron Rad.* **8**, 18–21.